Supplemental Material

Table of Contents

Supplemental Data

DNA-binding pore residues are important for substrate affinity

To determine if the crystals captured a physiologically-meaningful initiator state, we used fluorescence-anisotropy to monitor the binding of a labeled dT_{25} oligonucleotide to wild-type DnaA and to mutant initiators containing substitutions in observed DNA-binding residues. Because ssDNA binding is strongly nucleotide-dependent[25], and to avoid complications that might arise from hydrolysis (which inactivates DnaA), assays were run in the presence of ADP•BeF_3, a non-hydrolyzable analog that closely mimics the properties of ATP[25]. Substitution of Arg190 and Lys188 with alanine reduced binding affinity by 2-fold and 5-fold, respectively (**Fig S4a**, **Table S4**). Charge reversal changes to these positions impacted binding even more severely, lowering affinity by almost an order of magnitude in both cases. Changing Val156 to alanine reduced binding 4-fold. Together, these findings indicate that the contacts we observe for DNA binding to DnaA are functionally important. Unfortunately, the most significant DnaA/ssDNA contact, from helix α6, could not be probed, as it arises from a helix dipole of the protein that was not readily amenable to mutagenesis.

Significantly, our mutations did not affect the ATP-dependent oligomerization properties of DnaA (as assessed by glutaraldyhyde crosslinking, **Fig S4b**), indicating that loss of affinity did not arise from assembly defects. Sequence comparisons show that the residues seen to coordinate ssDNA (except Thr191) are highly conserved among bacterial initiators (**Fig S5**), with naturally-occurring substitutions at positions Arg190, Lys188 and Val156 exhibiting the same charge or hydrophobic characteristics across most species[15, 25]. Moreover, mutations of the same positions in *E. coli* DnaA (amino acids Arg245, Lys243 and Val211) also disrupt ssDNA binding and origin melting[15].

Supplemental References

61. Diederichs, K. & Karplus, P. A. Improved R-factors for diffraction data analysis in macromolecular crystallography. *Nat. Struct. Biol.* **4**, 269-275 (1997).
62. Davis, I. W. *et al*. MolProbity: all-atom contacts and structure validation for proteins and nucleic acids. *Nucleic Acids Res.* **35**, W375-83 (2007).
63. Lu, X. J. & Olson, W. K. 3DNA: a software package for the analysis, rebuilding and visualization of three-dimensional nucleic acid structures. *Nucleic Acids Res.* **31**, 5108-5121 (2003).

Supplemental Tables

Table S1 – Data collection and refinement statistics for DnaA-dA_{12} complex.

Data Collection	**Native**
Resolution	50-3.35
Wavelength, Å	1.1159
Space group	$P2_12_12_1$
Unit cell dimensions, Å	99.8, 114.2, 201.3
I/σ[a]	13.5 (2.0)
% R_{sym}[a]	8.8 (61.2)
% $R_{p.i.m.}$[a]	5.4 (38.6)
% Completeness[a]	98.9 (99.6)
Redundancy[a]	3.5 (3.6)
No. of reflections (unique)	113789 (32862)
Refinement statistics (43.49-3.37 A)	
No. of reflections (working/test set)	32802 / 1663
% R_{work} / % R_{free}	24.90 / 26.82
rmsd bonds (Å)	0.009
rmsd angles (°)	0.864
Ramachandran[d] -Preferred (%)	98.3
-Allowed (%)	1.7
-Outliers (%)	0
Number of atoms	10,874
Protein	10,477
Ligands	375
Waters	22
B-factors -Protein	109
-AMPPCP/Mg^{2+}	68
-dA_{12}	136

[a] Numbers in parentheses refer to highest resolution shell.
[b] $R_{p.i.m.}$ calculated as described in[61].
[c] $R_{work} = \sum||F_o| - |F_c||/\sum|F_o|$. R_{free} is calculated using 5% of the data omitted from refinement.
[d] As reported by Molprobity[62].

Table S2 – ssDNA (dA_{12}) local base step parameters* as seen in the crystal:

From->to:	Shift (Å)	Slide (Å)	Rise (Å)	Tilt (°)	Roll (°)	Twist (°)
A1 -> A2	1.7	1.12	3.02	9.35	6.58	42.35
A2 -> A3	1.84	0.1	3.75	-2.63	8.6	47.4
A3 -> A4	**-11.95**	**-5.05**	**5.69**	**-20.34**	**-16.11**	**-49.56**
A4 -> A5	1.92	1.15	2.95	9.65	10.51	45.87
A5 -> A6	1.82	0.08	3.77	-3.77	8.89	45.27
A6 -> A7	**-12.2**	**-4.76**	**5.11**	**-24.52**	**-4.39**	**-50.49**
A7 -> A8	1.78	0.83	3	10.83	-2.24	47.37
A8 -> A9	1.73	0.49	3.28	4.4	7.6	45.72
A9 -> A10	**-12.1**	**-5.29**	**6.53**	**-29.71**	**-14.64**	**-50.93**
A10 -> A11	2.07	0.81	3.12	7.62	3.24	47.63
A11 -> A12	1.58	0.34	3.53	3.73	2.31	44.69

*Calculated with the progam 3DNA[63]. Gaps between triplets are highlighted in bold.

Table S3 – DNA substrates used for studies.

Name	Sequence	Study
dA_{12}[a]	5′- AAAAAAAAAAAA – 3′	X-ray
F-dT_{25}[b]	5′- [Fl] TTTTTTTTTTTTTTTTTTTTTTTTT – 3′	Binding
FR-dT_{21}[b]	5′- [Cy5] TTTTTTTTTTTTTTTTTTTT [Cy3] – 3′	Extension
C3-dT_{21}[b]	5′- TTTTTTTTTTTTTTTTTTTT [Cy3] – 3′	Extension
15mer-TOP[c]	5′- TAGTACGTCTTATCT – 3′	Displacement
15mer-BOT[c]	5′- TCTTACTTAGTCGTA – 3′	Displacement
C3-15mer-BOT[c]	5′- TCTTACTTAGTCGTA [Cy3] – 3′	Displacement
20mer-TOP[c]	5′- AGACGTAGTACGTCTTATCT – 3′	Displacement
20mer-BOT[c]	5′- AGATAAGACGTACTACGTCT – 3′	Displacement
C3-20mer-BOT[c]	5′- AGATAAGACGTACTACGTCT [Cy3] – 3′	Displacement
30mer-TOP[c]	5′- TAGTACGTCTTATCTTCTTACTTAGTCGTA – 3′	Displacement
30mer-BOT[c]	5′- TACGACTAAGTAAGAAGATAAGACGTACTA – 3′	Displacement
C3-30mer-BOT[c]	5′- TACGACTAAGTAAGAAGATAAGACGTACTA [Cy3] – 3′	Displacement

[a] Obtained from Elim Biopharmaceuticals.
[b] Obtained from Integrated DNA Technologies.
[c] Obtained from Sigma-Aldrich.

Table S4 – ssDNA binding mutations.

Mutation	Nucleotide	$K_{d,app}$ (μM)	vs. WT
WT	ADP•BeF_3	0.11 ± 0.03	1
R190A	ADP•BeF_3	0.19 ± 0.05	1.7
V156A	ADP•BeF_3	0.40 ± 0.1	3.6
K188A	ADP•BeF_3	0.50 ± 0.1	4.5
R190D	ADP•BeF_3	0.88 ± 0.2	8
K188D	ADP•BeF_3	0.90 ± 0.2	8.2

Table S5 – Fluorescence properties of labeled DNA substrates and controls.

Sample	Fluorescence (au)/ Absorbance (OD) * f_{abs}	Φ_D	R_o (Å)	Efficiency (%)	Distance (Å)
Rhodamine 6G in EtOH	1255.5	0.95 (0.95)	N.A.	N.A.	N.A.
Fluorescein in 0.1 M NaOH	1290.3	0.98 (0.95)	N.A.	N.A.	N.A.
DnaA Buffer	21.6	0.016	52	57.6	49
DnaA ADP	N.A.	0.056	64	70.1	56
DnaA ADP•BeF_3	N.A.	0.13	73	18.4	94
DnaA-V156A	N.A.	0.14	74	68.7	65
DnaA-K188D	N.A.	0.092	69	54.9	67
DnaA-R190D	N.A.	0.13	73	79.6	58
DnaA-G281Q	N.A.	0.078	63	55.3	61
DnaA-S350D	N.A.	0.14	74	63.5	68
DnaA-R230A	N.A.	0.058	64	76.1	53
RecA Buffer	25.3	0.019	53	63.8	48
RecA-ADP	N.A.	0.11	71	49.5	71
RecA-ATPγS	N.A.	0.18	77	14.5	104

N.A. – Not Applicable.

Table S6 – FRET-based distance measurements.

DnaA	ADP	ADP•BeF_3
Efficiency	70%	18%
Distance	56 Å	94 Å
Distance from Structure		102 Å

RecA	ADP	ATPγS
Efficiency	49%	14%
Distance	71 Å	104 Å
Distance from Structure		109 Å

Supplemental Figures

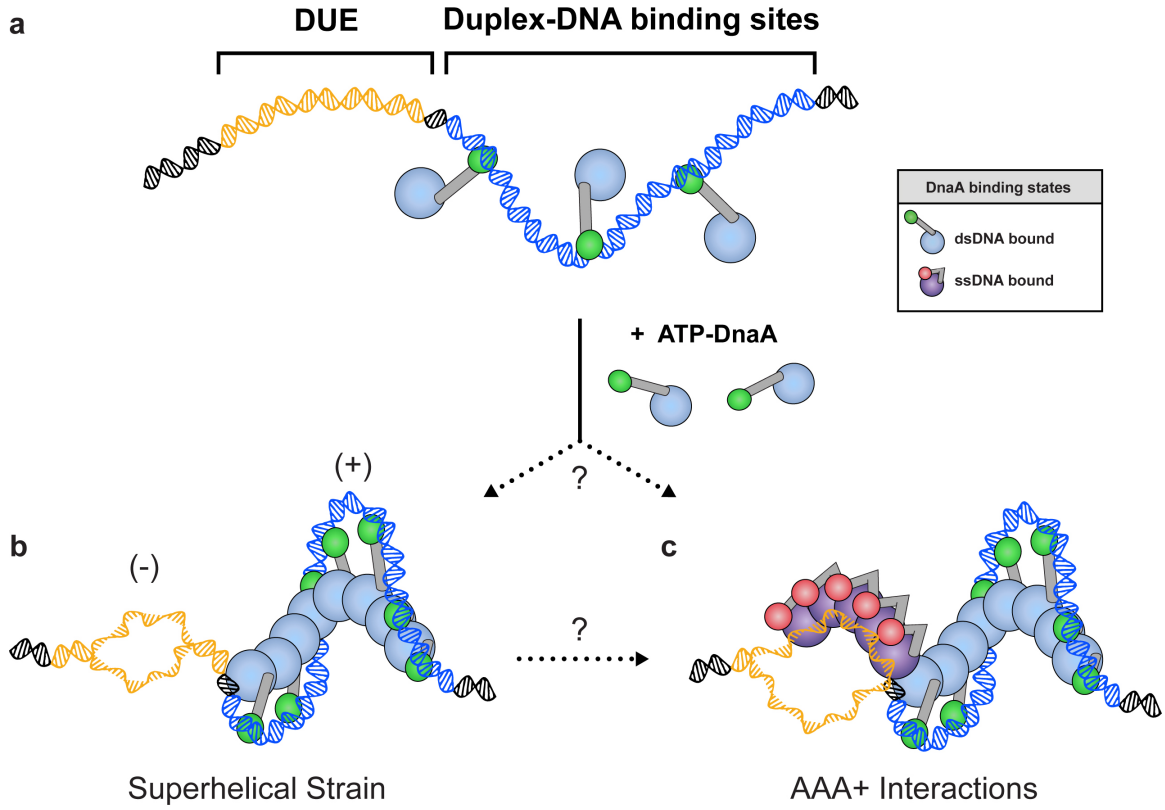

Figure S1 – **Possible mechanisms for origin melting by DnaA**. Two types of DnaA structural states have been proposed to exist depending on nucleotide and DNA binding status. **a,** DnaA monomers (state 1 - blue oval (N-terminal and AAA+ regions) and green oval (duplex-DNA-binding domain)) bind dsDNA (double-stranded DNA) regions (blue) in *oriC*. In the presence of ATP, DnaA self-assembles, wrapping DNA and melting the DUE (orange) by: **b,** introducing negative superhelical strain; **c,** through AAA+ ATPase domain interactions; or both. To bind ssDNA, DnaA has been proposed to adopt a second state (state 2 - purple oval (N-terminal and AAA+ regions) and red oval (duplex DNA binding domain)) in which the ATPase elements contact nucleic acid segments.

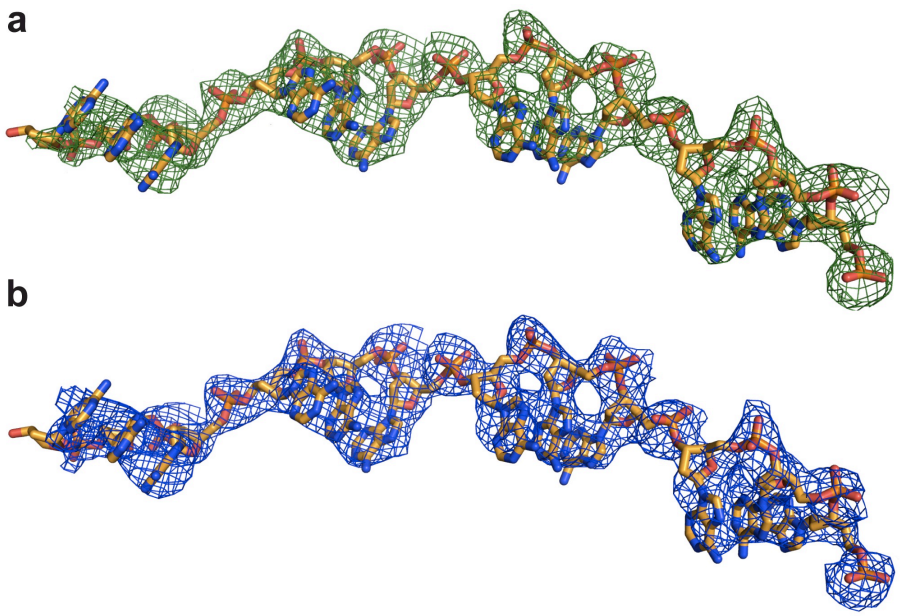

Figure S2 – **Electron density for single-stranded DNA**. **a,** F_o-F_c electron density (green, 1.5σ contour) from refinement with the DNA omitted. The refined model is in orange. **b,** $2F_o$-F_c electron density (blue, 1.2σ contour) from the model refined with DNA.

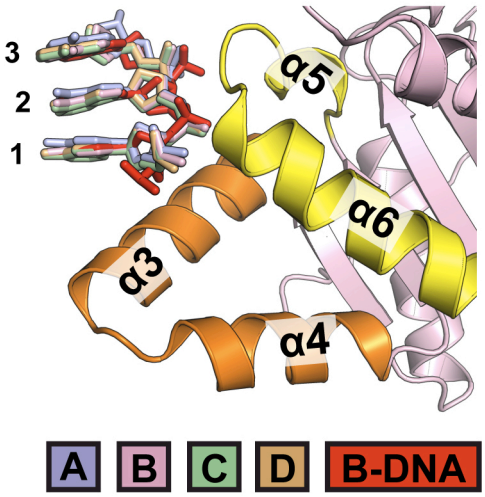

Figure S3 – **Alignment of trinucleotide segments**. Structural superposition of protein chains A, C and D onto chain B with the corresponding nucleotide triplets of bound ssDNA differentially colored to match the protein chains as shown in **Fig 1a**. Triplet numbering corresponds to **Fig 1d**.

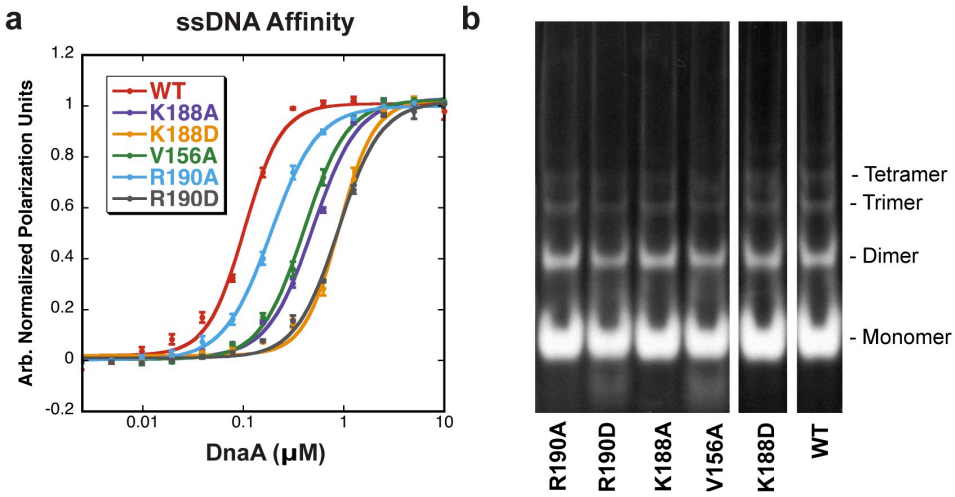

Figure S4 – **Single-stranded DNA binding mutants of DnaA**. **a,** Observed ssDNA contacts are important for affinity. Binding of F-dT_{25} by DnaA and ssDNA-binding site mutants (in the presence of ADP•BeF_3), monitored as a function of protein concentration by fluorescence polarization. Data were normalized so that the bottom and top plateaus are at zero and one, respectively. Error bars represent the standard deviation of three independent measurements. **b,** Oligomerization characteristics of ssDNA binding mutants. Indicated DnaA mutants were treated with glutaraldehyde and the resulting cross-linked species separated on a denaturing polyacrylamide gel as described previously[25].

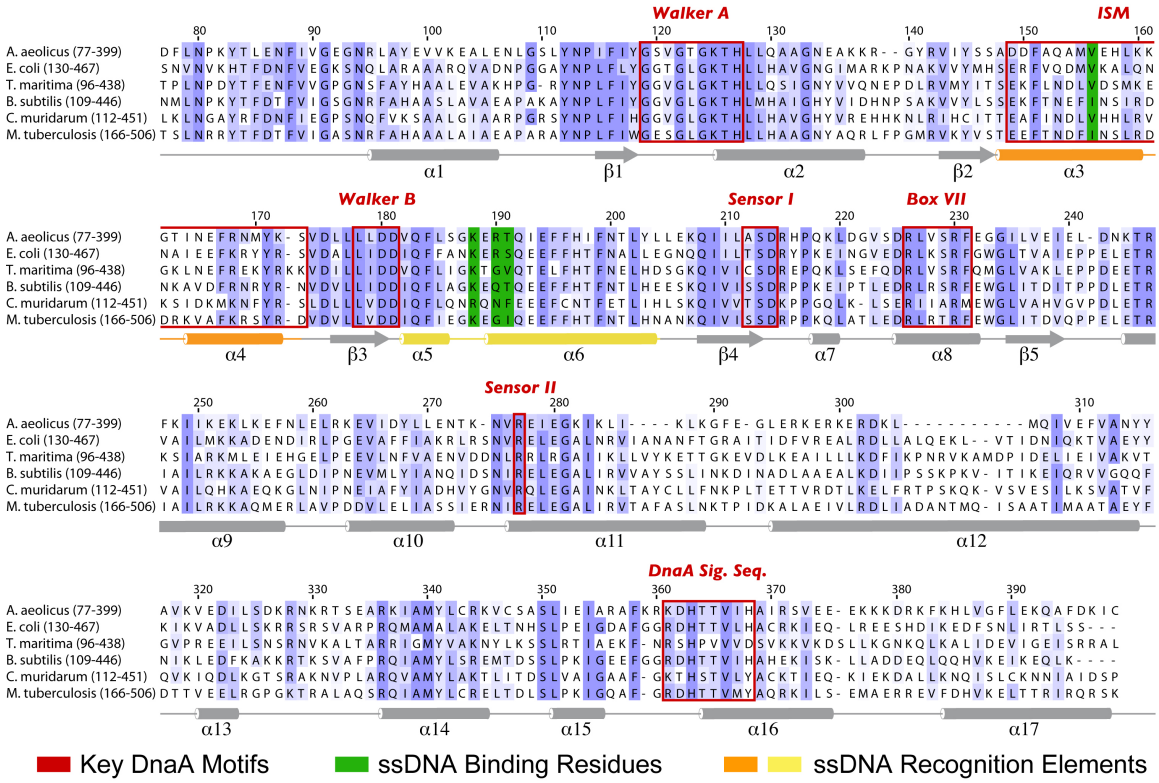

Figure S5 – **Multiple sequence alignment showing ssDNA binding residues**.

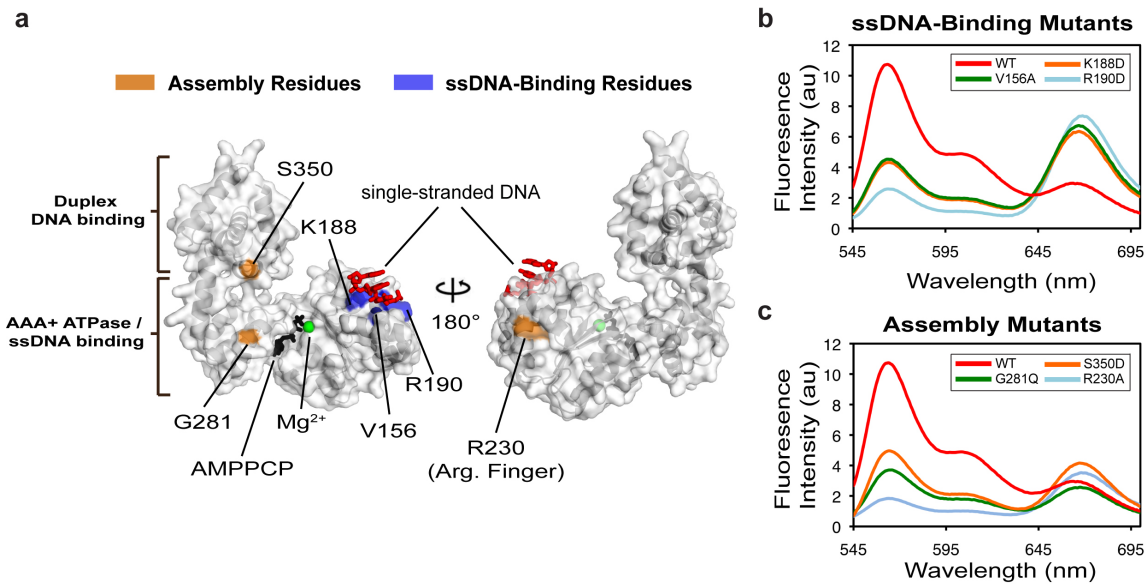

Figure S6 – **Extension assays for DnaA proteins containing ssDNA/assembly mutations**. **a,** Surface views of DnaA interfaces with mutated residues labeled and color-coded based on their role in assembly and ssDNA-binding (orange and blue, respectively). Assembly mutants tested: the arginine-finger mutant R230A, the AAA+/AAA+ interface mutant G281Q, and the DBD/AAA+ interface mutant S350D. **b, c,** Emission scan (donor excitation) for FR-dT_{21} in the presence of 10 μM of various DnaA mutants and wild-type. All experiments were conducted in the presence of ADP•BeF_3.

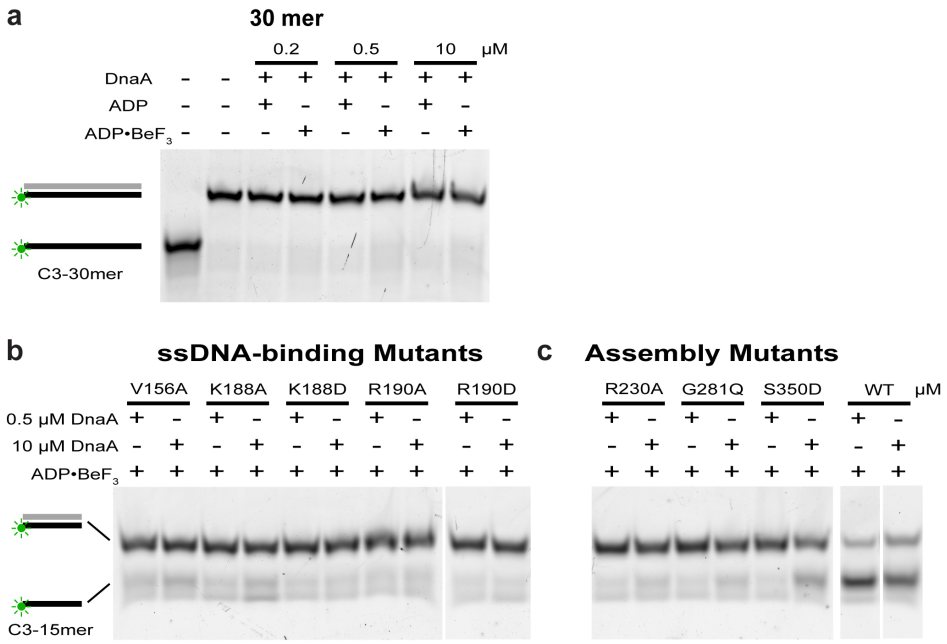

Figure S7 – **DNA strand displacement assays**. **a,** Lack of unwinding of a 30mer duplex substrate (C3-30mer). **b,** ssDNA-binding mutants fail to unwind a 15mer duplex substrate (C3-15mer). **c,** DnaAs assembly mutants fail to unwind a 15mer duplex substrate (C3-15mer). Wild-type unwinding is included for reference. The surface locations of tested mutants can be seen in **Fig S6a**. The DnaA concentrations used are indicated above each lane. Substrate sequences can be found in **Table S3**.

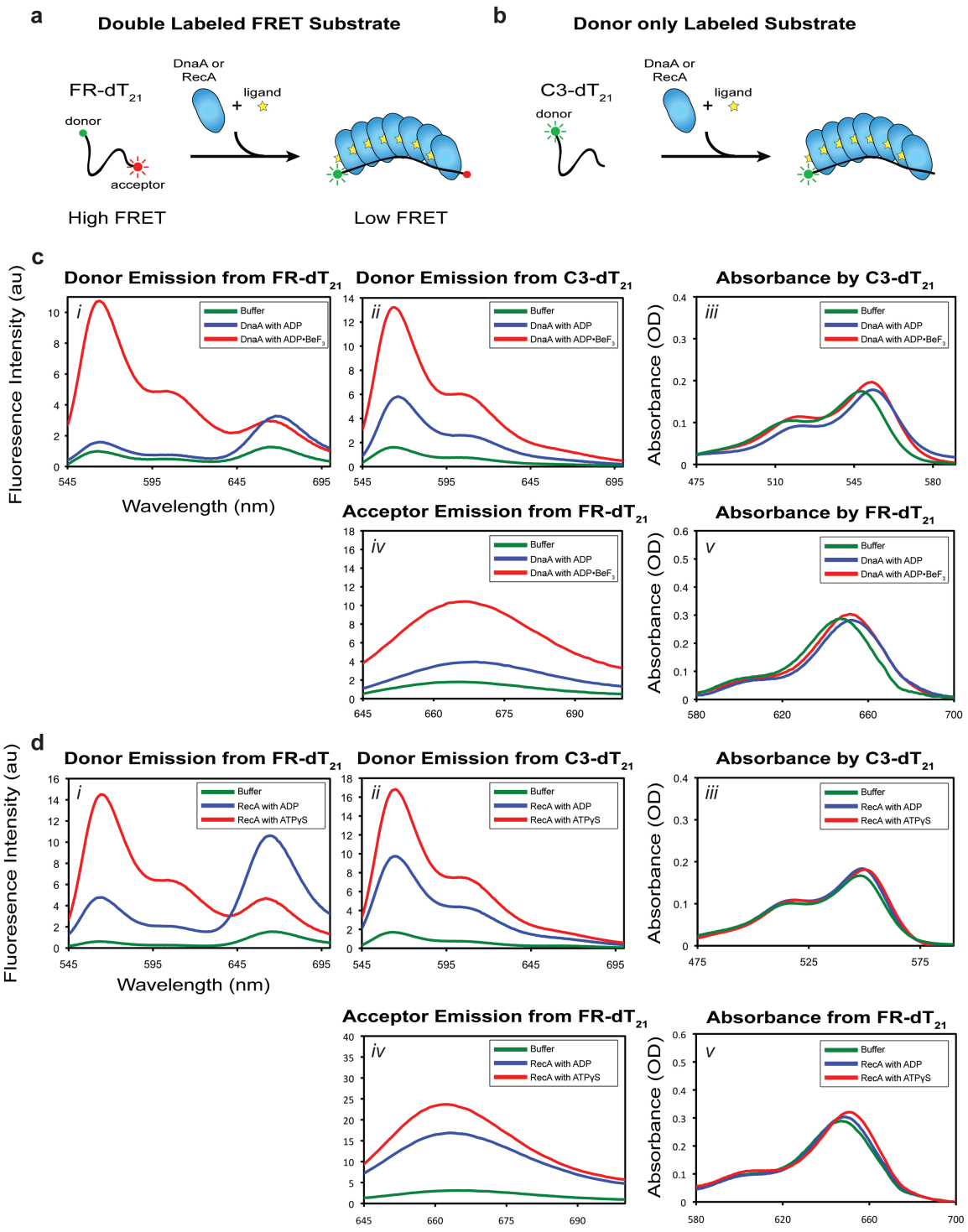

Figure S8 – **Fluorescence properties of labeled single-stranded DNA substrates in the presence of DnaA and RecA, with or without nucleotide present**. **a,** Cartoon of ssDNA extension assay with a donor-and-acceptor labeled substrate (FR-dT$_{21}$). **b,** Cartoon of ssDNA extension assay with a donor-only labeled substrate (C3-dT$_{21}$). **c,** Comparison of the effects of various DnaA-

free or nucleotide-bound DnaA-present reaction conditions on: ***i*,** Donor emission from FR-dT_{21}; ***ii*,** Donor emission from C3-dT_{21}; ***iii*,** Absorbance by C3-dT_{21}; ***iv*,** Acceptor emission from FR-dT_{21}; and ***v*,** Acceptor absorbance by FR-dT_{21}. **d,** Comparison of the effects of various RecA-free or nucleotide-bound RecA-present reaction conditions on: ***i*,** Donor emission from FR-dT_{21}; ***ii*,** Donor emission from C3-dT_{21}; ***iii*,** Absorbance by C3-dT_{21}; ***iv*,** Acceptor emission from FR-dT_{21}; ***v*,** Acceptor absorbance by FR-dT_{21}. We note that ADP-bound RecA stimulates acceptor emission more significantly than ADP-bound DnaA, possibly due to greater ssDNA binding by ADP-bound RecA. All donor emission scans were conducted with excitation at 530 nm, while acceptor emission scans were conducted with excitation at 630 nm.

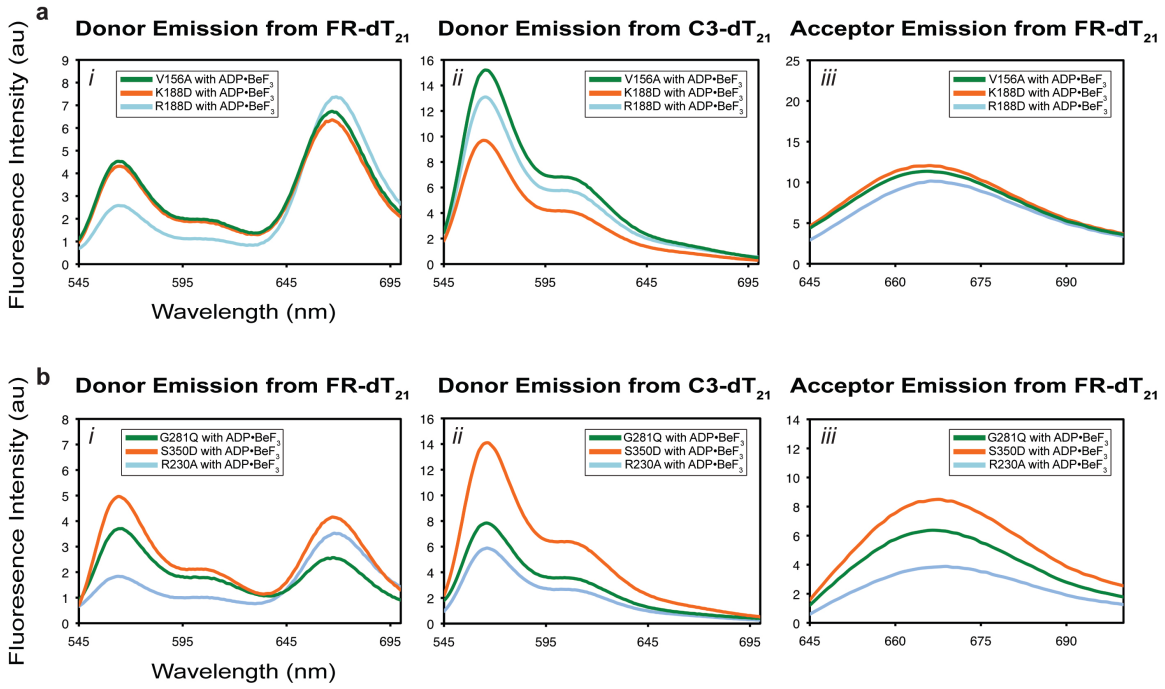

Figure S9 a, Fluorescence properties of labeled DNA substrates in the presence of mutant DnaA proteins defective for single-stranded DNA binding in the presence of ADP•BeF_3: ***i*,** Donor emission from FR-dT_{21}; ***ii*,** Donor emission from C3-dT_{21}; ***iii*,** Acceptor emission from FR-dT_{21}. **b,** Fluorescence properties of labeled DNA substrates in the presence of mutant DnaAs defective for assembly in the presence of ADP•BeF_3: ***i*,** Donor emission from FR-dT_{21}; ***ii*,** Donor emission from C3-dT_{21}; ***iii*,** Acceptor emission from FR-dT_{21}. All donor emission scans were conducted with excitation at 530 nm, while acceptor emission scans were conducted with excitation at 630 nm.

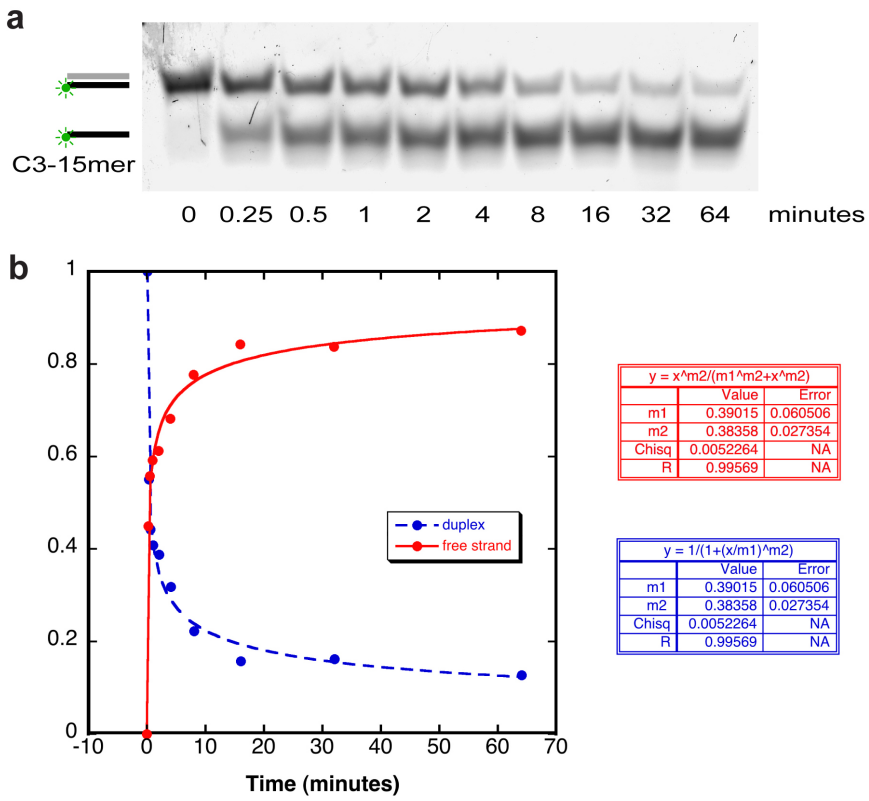

Figure S10 a, Time course of DnaA duplex melting of 15mer duplex substrates (C3-15mer). The duplex substrate and capture strand were added at time zero. Duplex melting experiments were conducted in the presence of 2 mM ADP•BeF_3 and 0.5 μM DnaA. **b,** Fraction of duplex and free strand within each lane normalized to one. Free-strand data were fit to a hyperbolic model; duplex data were fit to an IC50 model.